Comparative life cycle assessment of renewable energy storage systems for net-zero buildings with varying self-sufficient ratios

Energy 290 (2024) 130041

Contents lists available at ScienceDirect

Energy

journal homepage: www.elsevier.com/locate/energy

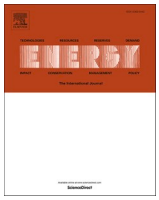

Comparative life cycle assessment of renewable energy storage systems for net-zero buildings with varying self-sufficient ratios

Son Tay Le [a], Tuan Ngoc Nguyen [a,*], Dac-Khuong Bui [a], Birch Teodosio [b], Tuan Duc Ngo [a,**]

[a] Department of Infrastructure Engineering, The University of Melbourne, Parkville, VIC 3010, Australia
[b] Energy Networks Australia, Melbourne, VIC 3000, Australia

ARTICLE INFO

Handling Editor: Dr X Zhao

Keywords:
Life cycle analysis
Building energy
Renewable energy system
Optimal sizing
Energy storage system
Hydrogen

ABSTRACT

The transition towards zero and net-zero buildings necessitates identifying sustainable and effective renewable energy systems to reduce the impacts of operational energy. This study analyses the environmental impacts of multiple microgrids that consist of a photovoltaic plant and a hybrid hydrogen/battery energy storage system in a grid-connected building. To this end, a three-step simulation process was proposed. The first step involved modelling the energy consumption of the building during operation. Following that, the size of components was optimised. Lastly, a comparative life cycle assessment was conducted to evaluate different self-sufficient ratios (SSR). The results show that as SSR increase, the optimised capacities of all components generally increase, although this relationship is complex, particularly as the system approaches full renewable capacity. The climate change impact initially decreases to its lowest values but then increase again towards achieving full self-sufficiency. Furthermore, the results highlight the importance of considering multiple environmental impact categories when designing renewable energy systems. A sensitivity analysis reveals that countries with carbon-intensive electricity grids can reduce climate change impacts by increasing their renewable energy penetration. However, for countries with a high proportion of renewable energy, a higher SSR may not lead to a lower climate change impact but rather exacerbate it.

1. Introduction

In recent years, climate change and global warming have emerged as critical global issues. The building sector is a major contributor to the total energy consumption (35 %) and global energy emissions (38 %) [1]. To address this problem, the concept of "zero energy" and "net-zero energy" buildings has been introduced. A net-zero energy building (NZEB) produces as much energy as it consumes over a year, while a zero energy building (ZEB) goes a step further and consumes zero energy from external sources on an annual basis [2]. The integration of solar and wind energy into building design can facilitate the construction of ZEBs or NZEBs, thereby reducing reliance on the grid [3]. Although the costs of these technologies have decreased dramatically over the past few years, one of the main challenges of renewable energy is its intermittency, which leads to a mismatch between energy supply and demand [4,5]. Therefore, an energy storage system (ESS) is essential to achieve a reliable and stable energy supply [6,7]. Storage capacity and discharge time are two main characteristics of energy storage technologies. Batteries are the most well-known electrochemical energy storage devices and have been widely used in transportation, electronics, and power grid applications. As a mature technology, the battery energy storage system (BESS) is flexible, reliable, economical, and responsive for storing energy [8,9]. However, with the increasing penetration of renewable energy and the gradual phase-out of grid connections, long-duration energy storage has become significantly more important [10,11]. Hydrogen has been identified as a key technological solution for addressing climate change because of its abundant availability, high mass-energy density, and pollution-free production process. A hydrogen energy storage system (HESS) converts energy into hydrogen using physical-based or material/chemical-based methods. The use of hydrogen as a clean fuel as well as a long-term energy storage option has been rapidly increasing [12]. In the context of the building sector, where achieving decarbonisation goals is crucial, it is anticipated that a substantial number of renewable energy systems will be introduced in the next few years [13]. To support this transition, both battery and hydrogen technologies are potential solutions for reducing carbon emissions [14,15].

* Corresponding author.
** Corresponding author.
E-mail addresses: tuan.nguyen@unimelb.edu.au (T.N. Nguyen), dtngo@unimelb.edu.au (T.D. Ngo).

https://doi.org/10.1016/j.energy.2023.130041
Received 29 June 2023; Received in revised form 21 October 2023; Accepted 16 December 2023
Available online 22 December 2023

Nomenclature

E_B^t	energy stored in the BESS at time t
E_H^t	energy stored in the HESS at time t
$P_{B\_charge}^t$	charge power of BESS at time t
$P_{B\_discharge}^t$	discharge power of BESS at time t
$P_{H\_charge}^t$	charge power of HESS at time t
$P_{H\_discharge}^t$	discharge power of HESS at time t
$P_{G,imp}^t$	power import from the grid at time t
P_L^t	load at time t
P_{PV}^t	output power from solar PV at time t
S_i	size of component i
SOC_i^t	state of charge of component i at time t
SOH_i^t	state of health of component i at time t
U_i	unit capital cost for component i
η_B	BESS efficiency
η_I	inverter efficiency
η_{EL}	electrolyser efficiency
η_{FC}	Fuel cell efficiency

Abbreviations

AP	acidification potential
APOS, S	Allocation at the point of substitution approach, system model
BESS	Battery Energy Storage System
CED	non-renewable energy consumption
Cut-off, S	Cut-off approach, system model
EOL	End-of-Life
EP	eutrophication potential
ESS	Energy Storage System
GLO	Global market
GWP	global warming potential
HESS	Hydrogen Energy Storage System
HVAC	heating, ventilation, and air conditioning
LCA	Life Cycle Analysis
LCI	Life Cycle Inventory
LCIA	Life Cycle Impact Assessment
LPSP	Loss Of Power Supply Probability
MOMFA	Multi-Objective Modified Firefly Algorithm
NPV	Net Present Value
PEMEL	electrolyser
PEMFC	proton exchange membrane fuel cells
POF	photochemical oxidant formation
RES	Renewable Energy Sources
SSR	Self Sufficiency Ratio
TEA	Techno-Economic Analysis

In recent years, there has been growing research interest in integrating ESSs in building and commercial applications, with a focus on reducing system costs. Zhang et al. [16] conducted a techno-economic analysis (TEA) on grid-connected systems integrated with BESS or HESS for building applications and found that the Net Present Value (NPV) can increase by approximately 50,000 SEK for BESS and 70,000 SEK for HESS. Ren et al. [17] proposed a residential energy system that can reduce the annual running cost, primary energy consumption, and CO_2 emissions by 70 %, 20 %, and 13 %, respectively, when compared with the conventional system without distributed generations or storage equipment. Chadly et al. [18] demonstrated that BESS and HESS are economically attractive for fully renewable buildings and can enhance the reliability and resiliency of power over the long term. Tahani et al. [19] investigated the integration of a PV/Wind/BESS system in a building located in Tehran with a focus on achieving fully renewable energy. They tested the system at different levels of loss of power supply probability (LPSP) and found that approaching a fully renewable system results in a slower payback time. Specifically, the payback time increases from 12.14 years at LPSP of 3.28 %–14.7 years at LPSP of 0 %. Gabrielli et al. [15,20] conducted a study on the design and operation of multiple buildings using BESS and HESS. The findings suggest that while fully renewable systems are an option, they need to be evaluated thoroughly, as they can result in substantially higher total annual costs. Similarly, Le et al. [21] employed BESS and HESS across different scenarios, ranging from partially to almost fully renewable systems. The study shows that the NPV rapidly decreases when the system approaches fully renewable. For instance, in Melbourne, Australia with a high season mismatch, at a self-sufficiency ratio (SSR) of 80 %, the NPV is 0.8 M USD, and it decreases to -8M USD at SSR 98 %.

On the other hand, the environmental impact of BESS and HESS has also been studied through life cycle analysis (LCA), which takes into account the environmental impacts associated with the entire life cycle of the ESS, including manufacturing, transportation, installation, operation, and end-of-life disposal. LCA is a systematic and quantitative methodology that can provide valuable information and guide decision-makers in making eco-friendly choices and promoting sustainability [6,22]. Several studies have used LCA to assess the environmental impact of BESS and HESS, including their carbon footprint, energy consumption, and waste generation. For off-grid applications, Belmonte et al. [23] designed a self-sufficient system for two days in the worst conditions and performed an LCA of BESS and HESS from the extraction of raw materials and fuels to their production, use, and disposal or recycling. Mendecka et al. [24] used LCA to analyse the environmental impact of off-grid HESS and BESS in commercial buildings located in eight climate zones in the United States. Bionaz et al. [13] and Gandiglio et al. [22] examined off-grid renewable systems with diesel generator backup, and assessed their environmental impacts using LCA. While Bionaz et al. [13] focused only on CO_2 emissions, Gandiglio et al. [22] considered 12 environmental impacts using the Environmental Footprint (EF) 3.0 method. For grid-connected applications, Peppas et al. [25] conducted an LCA of a hybrid PV/wind/HESS system for an office building in Greece and found that the hybrid energy system resulted in a significant reduction in different environmental impact indicators compared with the exclusive use of the Greek energy grid mix for electricity, which still heavily relies on fossil fuels. The study found that the hybrid energy system resulted in a 40 % reduction in global warming potential and a 42 % and 35 % reduction in acidification potential and photochemical ozone creation potential, respectively, indicating it as a promising and environmentally sound solution for the building sector. Di Florio et al. [26] focused on the environmental impact of a grid-connected single--family house using only hydrogen. The study emphasizes the cleanliness of the Italian grid in assessing the environmental performance of the nano-grid and found that a nano-grid powered entirely by photovoltaic energy could reduce CO2 equivalent emissions by up to 68 % compared to a nano grid with the current Italian energy mix. Thus, efforts to increase the use of renewable energy sources in the national energy production can have a significant positive impact on the environmental performance of residential hydrogen-powered systems. Rossi et al. [27] conducted an LCA for PV systems with different HESS and BESS technologies in residential applications. The study assessed the connection of the home system to a grid and found it to be a more sustainable option than other off-grid solutions. While 700 bar hydrogen storage was the best off-grid configuration for minimising environmental impact (37.77 Pt s/MWh), an efficient connection with a grid even resulted in a lower environmental impact (22.81 Pt s/MWh). This finding is significant because it suggests that a future renewable energy system (RES) should

balance grid connectivity and energy storage to maximise sustainability and reduce the environmental impact.

The literature review of the relevant studies integrating ESSs in building and residential applications is summarised in Table 1. Although there are booming research and practices in this area, several research gaps have been identified.

(1) TEA studies have demonstrated that integrating ESSs into building applications can lead to emission reductions and economic benefits. However, a balanced approach between on-site renewable generation and the grid is crucial, as transitioning to a fully renewable building can incur significant costs. Furthermore, it is worth noting that in some TEA studies, the environmental impact was evaluated using simple metrics such as the amount of kg CO_2 emissions per litre of diesel consumption or the carbon intensity of grid electricity in kg CO_2 per kWh. An environmental analysis of the capital components of these systems is typically not considered. Therefore, there is a need of research to consider a more comprehensive analysis of the environmental impact of ESSs on the system life cycle.
(2) LCA has been widely used to evaluate the environmental impacts of ESS in buildings and residential applications, but most previous studies have only examined single configurations under a specific LPSP, which were pre-optimised or designed. Achieving optimal long-term sustainability, in the long run, requires a careful balance between renewable energy use and grid dependence.
(3) While previous studies have focused on the economic and operation of ESSs at different SSR, there is currently a lack of comprehensive environmental assessments using LCA. In contrast, LCA studies have typically examined a single system, overlooking the balanced approach between on-site renewable generation and the grid. Thus, there is still a lack of systematic methodology to evaluate and compare the environmental impact across different levels of production and utilization.

Table 1
Summary of the relevant studies integrating ESSs in building and residential applications.

Ref	Scope	LCA	Environmental analysis remarks[a]
Zhang et al. [16]	Multiple systems with different SSR		Focus on TEA, no environmental analysis
Ren et al. [17]	Single system		Focus on TEA, CO_2 emission is simplified as the sum of electricity and gas imported from the grid
Chadly et al. [18]	Single system		Focus on TEA, no environmental analysis
Tahani et al. [19]	Multiple systems with different SSR		Focus on TEA, no environmental analysis
Gabrielli et al. [15, 20]	Multiple systems with different SSR		Focus on TEA, CO_2 emission is simplified as the sum of electricity and gas imported from the grid
Le et al. [21]	Multiple systems with different SSR		Focus on TEA, no environmental analysis
Belmonte et al. [23]	Single system	✔	2 impact categories (GWP, CED)/cradle-to-gate
Mendecka et al. [24]	Multiple systems at different location	✔	4 impact categories (GWP, AP, EP, CED)/cradle-to-grave
Bionaz et al. [13]	Single system	✔	Only GWP/cradle-to-grave
Gandiglio et al. [22]	Single system	✔	12 impact categories/cradle-to-utilization
Peppas et al. [25]	Single system	✔	3 impact categories (GWP, AP, POF)/cradle-to-gate
Di Florio et al. [26]	Single system	✔	18 impact categories/cradle-to-grave
Rossi et al. [27]	Multiple systems with different technologies	✔	Single score impact values/cradle-to-grave

[a] GWP: global warming potential; AP: acidification potential; EP: eutrophication potential; CED: non-renewable energy consumption; POF: photochemical oxidant formation.

To address the aforementioned research gaps, a systematic methodology was proposed in this study. The main contributions and innovation of the paper are as follows.

(1) This study conducts a comprehensive LCA of multiple systems operating at various SSRs. This approach provides valuable insights into the environmental effects associated with the integration of RES in buildings.
(2) This study introduces a novel three-stage simulation methodology to evaluate the environmental impacts of microgrids. These microgrids consist of PV system and a hybrid hydrogen/battery energy storage system, integrated into grid-connected buildings. This method involves the following sequential steps: modelling the energy demand with Energy Plus, optimising components with MATLAB, and performing LCAs with SimaPro.
(3) To assess climate change's sensitivity to different grid compositions, a sensitivity analysis was performed to assess the impact of different grid mixes. In addition to the global mix, grid mixes with higher/lower carbon footprints are selected for the sensitivity analysis, highlighting the impact of different energy sources in the grid.

Thus, the innovation and global significance of this study lie in its methodological approach and its implications for the broader research and industry audience. Firstly, this study introduces a novel three-stage simulation methodology serves as an innovative framework for researchers and practitioners in the field, introducing a systematic approach to assess the sustainability of ESS integration from energy demand modelling to life cycle assessments in building applications. Secondly, this study addresses a critical global concern—sustainable energy transition. Nations worldwide commit to reducing carbon emissions and promoting renewable energy sources; hence, the findings on the environmental impacts of transitioning to fully renewable buildings have immediate relevance for policymakers, industry leaders, and environmental organisations, as they provide insights to balancing on-site renewable energy generation with energy consumption from the grid. The remainder of this paper is organised as follows. Section 2 describes the three-stage simulation procedure employed in this study. The results and discussion are presented in Section 3. Section 4 concludes the findings of the study.

2. Methodology

Fig. 1 provides an overview of the three-step simulation process used in this study. At the beginning of this process, unlike our previous study [21], where the load profile of an actual warehouse was measured, the electricity demand of a three-floor office building in this study was modelled in Energy Plus. Details of the building model in EnergyPlus are provided in Section 2.1. In the second step, the total energy consumption is imported to MATLAB to design the RES based on the framework presented by Le et al. [21]. An optimisation algorithm in MATLAB is used to determine the optimal capacity and breakdown of the load coverage for a set of different SSRs. The optimisation strategies employed in this study are described in Section 2.2. The final step involves conducting multiple LCAs in SimaPro using various scenarios, each with different component capacities (optimised in the previous step) and derived load coverage. The life cycle analysis framework employed in this study is described in Section 2.3.

2.1. Building energy analysis

The case study considered in this analysis is a three-floor office building that serves as a benchmark model for the Department of Energy

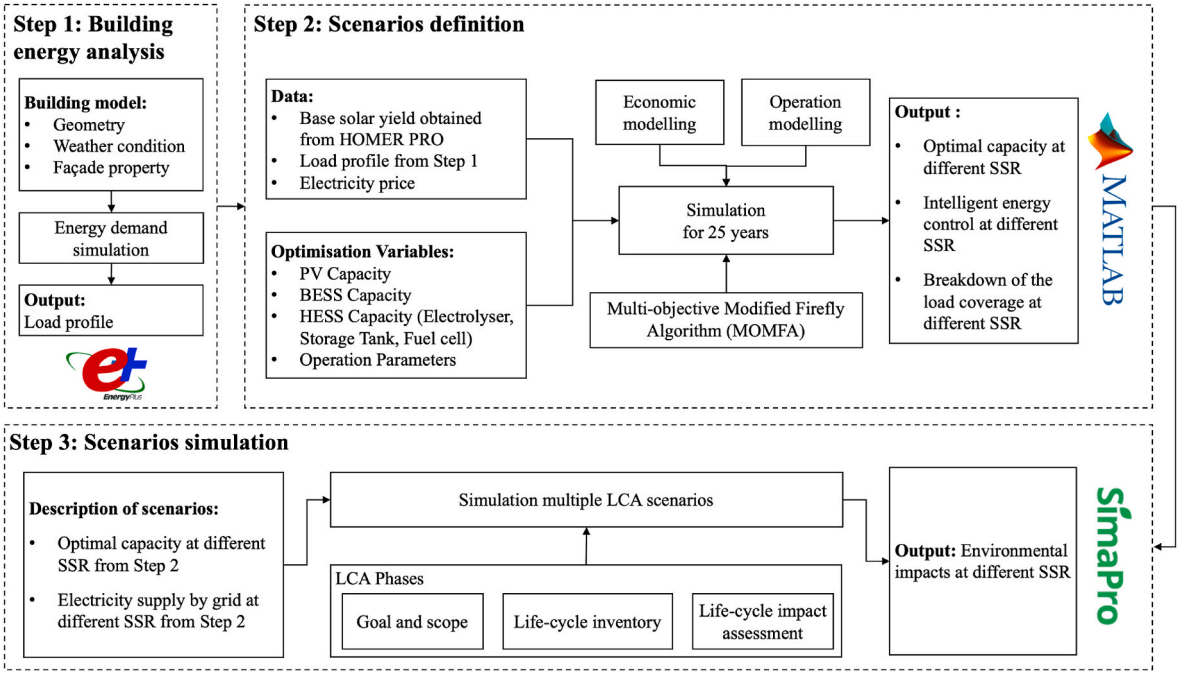

Fig. 1. Flowchart of the simulation process for life cycle assessment of renewable energy systems with varying self-sufficient ratio (SSR).

[28,29]. The building is modelled in EnergyPlus software to obtain the operational energy of the building. The building has windows on all four sides with a window-to-wall ratio of 60 % and a total floor area of 4982 m^2, as shown in Fig. 2. The windows on each side of the building are conventional low-emittance windows with a U-value of 3.228 W/m^2K, solar heat gain coefficient of 0.229, and visible transmittance of 0.189.

Simulations are conducted in EnergyPlus, assuming a typical working day of 8:00 to 17:00 with lighting scheduled to be on during working hours. The heat gain per floor area for lights is assumed to be 12.9 W/m^2, and a minimum workplace illuminance at the work plan level is maintained at 500 lx to ensure sufficient lighting for occupants. The heating, ventilation, and air conditioning (HVAC) system used in this case study is a Packaged Variable Air Volume air loop system consisting of a pre-assembled air handling unit that includes a fan, filters, and a cooling coil. The airflow rate in the system can be adjusted based on the heating and cooling demands of each zone or room, which results in energy savings and improved indoor air quality. Furthermore, the heating temperature setpoints for the HVAC system are defined at 18 °C and 15 °C during working and non-working hours, respectively, based on common practices within the energy sector. The choice of 18 °C for heating point is grounded on the presumption of negligible energy consumption for heating or cooling between mean daily temperatures [30]. On the other hand, the cooling temperature setpoints are set at 25 °C for working hours and 28 °C for non-working hours, aligning with industry standards. The temperate of 25 °C is stipulated as the summer indoor design temperature, a well-acknowledged standard within the HVAC community for maintaining indoor comfort and managing energy consumption during warmer months [31]. The extended range of cooling and heating setpoints during non-working hours is primarily aimed at reducing energy consumption, as buildings have fewer or no occupants during these times, allowing for more flexible temperature settings without compromising comfort.

The building is located in Melbourne, Australia which has a marine west coast climate with four distinct seasons: spring, summer, autumn, and winter. The summer and winter average temperatures are 19.8 °C and 10.5 °C, respectively. The weather station used in this study is located at 37°49′ South and 144°58′ East with an elevation of 32 m above sea level. At a time-step of 1 h, the simulation determines the yearly energy usage of the office building, including heating, cooling, and lighting. The yearly energy usage is assumed to remain consistent throughout the 25-year period [16,32].

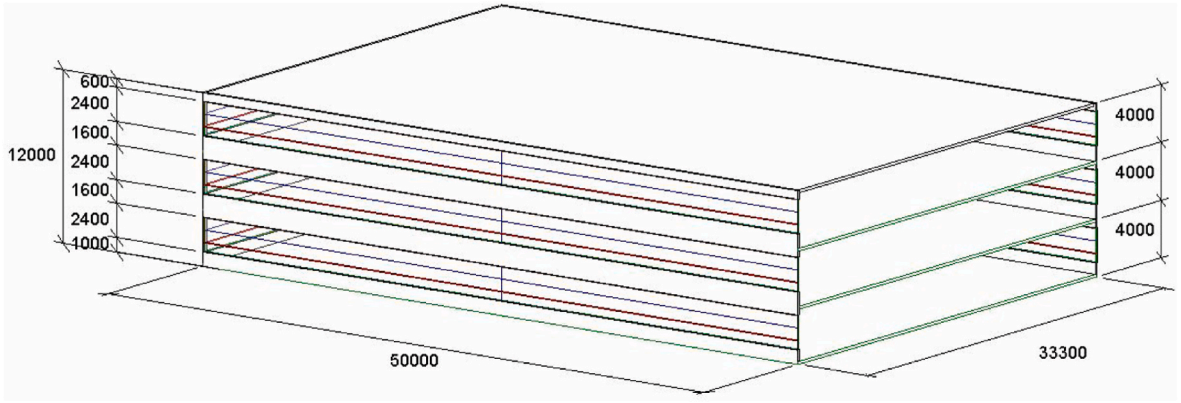

Fig. 2. Case study: A medium office model [29], units in mm.

2.2. Simulation of ESS and operation

Fig. 3 illustrates a schematic diagram of the RES installed to offset the operational energy in the building, which is obtained in the previous section. The system primarily relies on rooftop photovoltaics (PV) to generate electricity. The PV system converts solar energy into direct current (DC), which is then transformed into alternating current (AC) using an inverter. To estimate the solar yield from the PV, the HOMER PRO Software [33] is used to determine the base solar power output. For more information on the functionalities and implementations of HOMER software, readers are advised to refer to Ref. [34]. The yield of the PV system is assumed to be linearly proportional to the base solar energy. This assumption is based on the PV system model used in previous studies [35–37]. In order to address the intermittency of the PV system, a hybrid storage system consisting of a BESS and a HESS is used in the building for storing the excess energy generated by solar panels. The hybrid system is chosen because of its techno-economic efficiency as evidenced in the previous study [21]. This superior performance is due to the synergistic combination of the two technologies, with hydrogen serving as a long-term energy storage solution and batteries utilised for short-term storage purposes. Based on the profiles of electrical load in Fig. 6, the design and operation of the RES are optimised over a time horizon of 25 years and with hourly resolution.

The following equation depicts the power of the system at time interval t:

For BESS:

$$P^t_{B\_charge} = max\left(P^t_{PV} - P^t_L, 0\right) \tag{1}$$

$$E^t_B = E^{t-1}_B + P^t_{B\_charge} \times \Delta t - P^t_{B\_discharge} \times \Delta t \tag{2}$$

$$P^t_{B\_discharge} = max\left(\frac{1}{\eta_B}\left(\frac{P^t_L}{\eta_I} - P^t_{PV}\right), 0\right) \tag{3}$$

For HESS:

$$P^t_{H\_charge} = max\left(\left[P^t_{PV} - P^t_L\right] \times \eta_{EL}, 0\right) \tag{4}$$

$$E^t_H = E^{t-1}_H + P^t_{H\_charge} \times \Delta t - P^t_{H\_discharge} \times \Delta t \tag{5}$$

$$P^t_{H\_discharge} = max\left(\frac{1}{\eta_{FC}}\left(\frac{P^t_L}{\eta_I} - P^t_{PV}\right), 0\right) \tag{6}$$

where the output power from the solar PV at time interval t is denoted as P^t_{PV}, and the load demand is denoted as P^t_L. $P^t_{B\_charge}$, E^t_B, and $P^t_{B\_discharge}$ are the charge power, energy stored, and discharge power of the BESS at interval time t, respectively. Similarly, $P^t_{H\_charge}$, E^t_H, and $P^t_{H\_discharge}$ are the power delivered from the electrolyser to the hydrogen storage tank, the energy stored in the tank, and the power that fuel cell supply to the building, respectively. It should be noted that either the BESS or HESS can operate at any time interval t, within which the system operates in either the charge or discharge mode. The efficiency (η) of each component is considered, including the inverter ($\eta_I = 97\%$), battery ($\eta_B = 95\%$), electrolyser ($\eta_{EL} = 80\%$), and fuel cell ($\eta_{FC} = 65\%$). A review of the literature was conducted to determine these efficiency values. Previous research has reported inverter efficiencies in the range of 95 %–97 % [38,39]. In this study, $\eta_I = 97\%$ is chosen to align with the higher end of these reported values. For the battery component, an initial efficiency of 95 % is based on experimental results [40]. For the electrolyser and fuel cell components, various modelling approaches are available in the literature. The first approach assumes a fixed efficiency, neglecting the impact of varying working conditions, while other more detailed methods consider factors such as current, voltage (activation loss, ohmic loss, etc.), pressure, and temperature. This research opted for the former approach which can be found in similar studies [35–37,41], acknowledging that the efficiency can indeed fluctuate based on the aforementioned factors, leading to variations in reported efficiencies in the literature. The chosen values of $\eta_{EL} = 80\%$, and $\eta_{FC} = 65\%$ in this study represent a midpoint between the varying efficiency values found

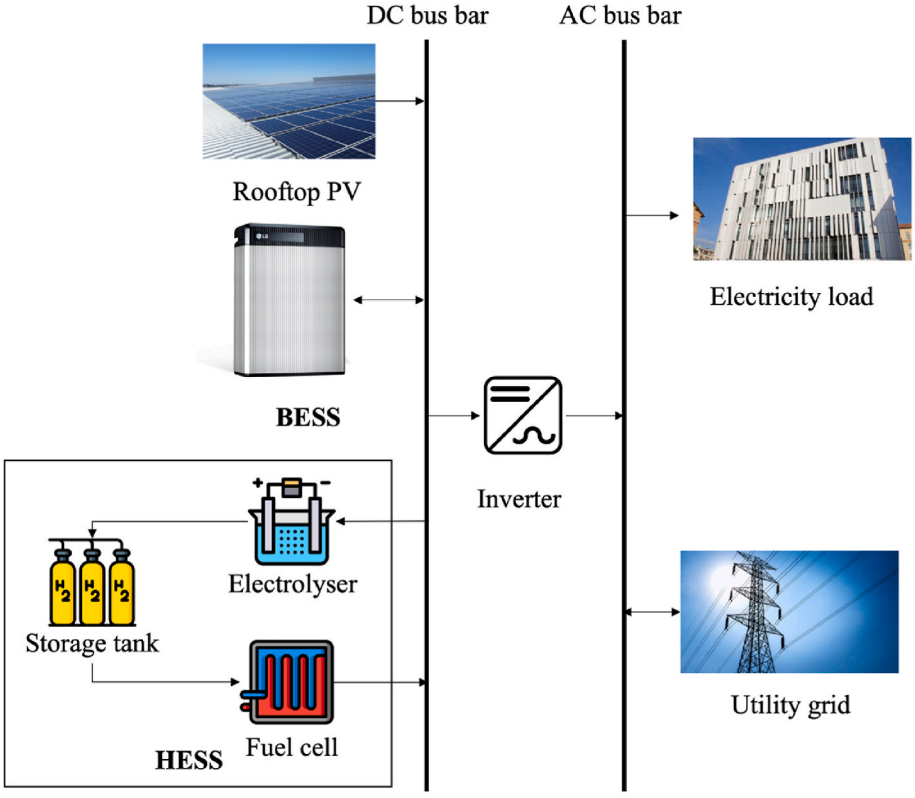

Fig. 3. System schematic layout of the grid-connected buildings.

in the literature.

The operational strategy used in this study is based on the framework proposed in our previous work [21]. In this strategy, the BESS is first charged, and once it is full, the electrolyser is charged. The fuel cell is operated when the battery becomes empty. The multi-objective modified firefly algorithm (MOMFA) is used to optimise the component sizing and operation variables of the ESS to maximise the NPV and SSR. While the NPV represents the economic incentives of the RES, the SSR is the percentage of the electricity demand supplied by the on-site RES over the total electricity demand:

$$SSR = \left(1 - \frac{\sum_{t=0}^{t=N} P_{G,imp}^{t}}{\sum_{t=0}^{t=N} P_{L}^{t}}\right) \times 100\% \quad (7)$$

Where $\sum_{t=0}^{t=N} P_{G,imp}^{t}$ and $\sum_{t=0}^{t=N} P_{L}^{t}$ is the total power imported from the grid and total energy demand over the 25-year period consisting of N time intervals (25×8760).

Fig. 4 summary the optimisation procedure used in this work. The procedure begins with the utilization of input data, which includes the hourly energy demands of a building obtained from the Energy Plus simulation in Section 2.1, solar output data from Melbourne using HOMER software, and various cost, specifications, and price information as detailed in our previous study [21]. An ultimate cost scenario is chosen for this study which is based on the cost target set by the International Energy Agency (IEA) [42] and the United States Department of Energy (DOE) [43,44]. Additionally, there are five optimisation variables which are the size of the PV system (S_{PV}), BESS (S_{BESS}), electrolyser ($S_{electrolyser}$), hydrogen tank ($S_{hydrogen\ tank}$), and fuel cell ($S_{fuel\ cell}$). Subsequently, for each year within the 25-year simulation period, dynamic factors such as electricity prices, solar and battery degradation, and anticipated O&M and replacement costs are computed. These data are then incorporated into the hourly energy modelling process, employing Eq. (1) through (6) to calculate both revenue and power imports from the grid for each year y. Ultimately, the NPV and the SSR of the system over the 25-year duration are determined. The MOMFA is a stochastic, nature-inspired optimisation algorithm, initially introduced by Yang [45], Chou and Ngo [46] and further developed in our previous works [21,47–49]. MOMFA generates an initial population of 14 fireflies, each representing a different system configuration with unique values for the five optimisation variables (S_{PV}, S_{BESS}, $S_{electrolyser}$, $S_{hydrogen\ tank}$ and $S_{fuel\ cell}$). These 14 systems undergo the 25-year simulation process illustrated in Fig. 4. For every iteration, the MOMFA continues adjusting positions of these fireflies to maximise two objective functions: NPV and SSR. A total of 400 iterations have been determined through sensitivity analysis to achieve a balance between accuracy and simulation time.

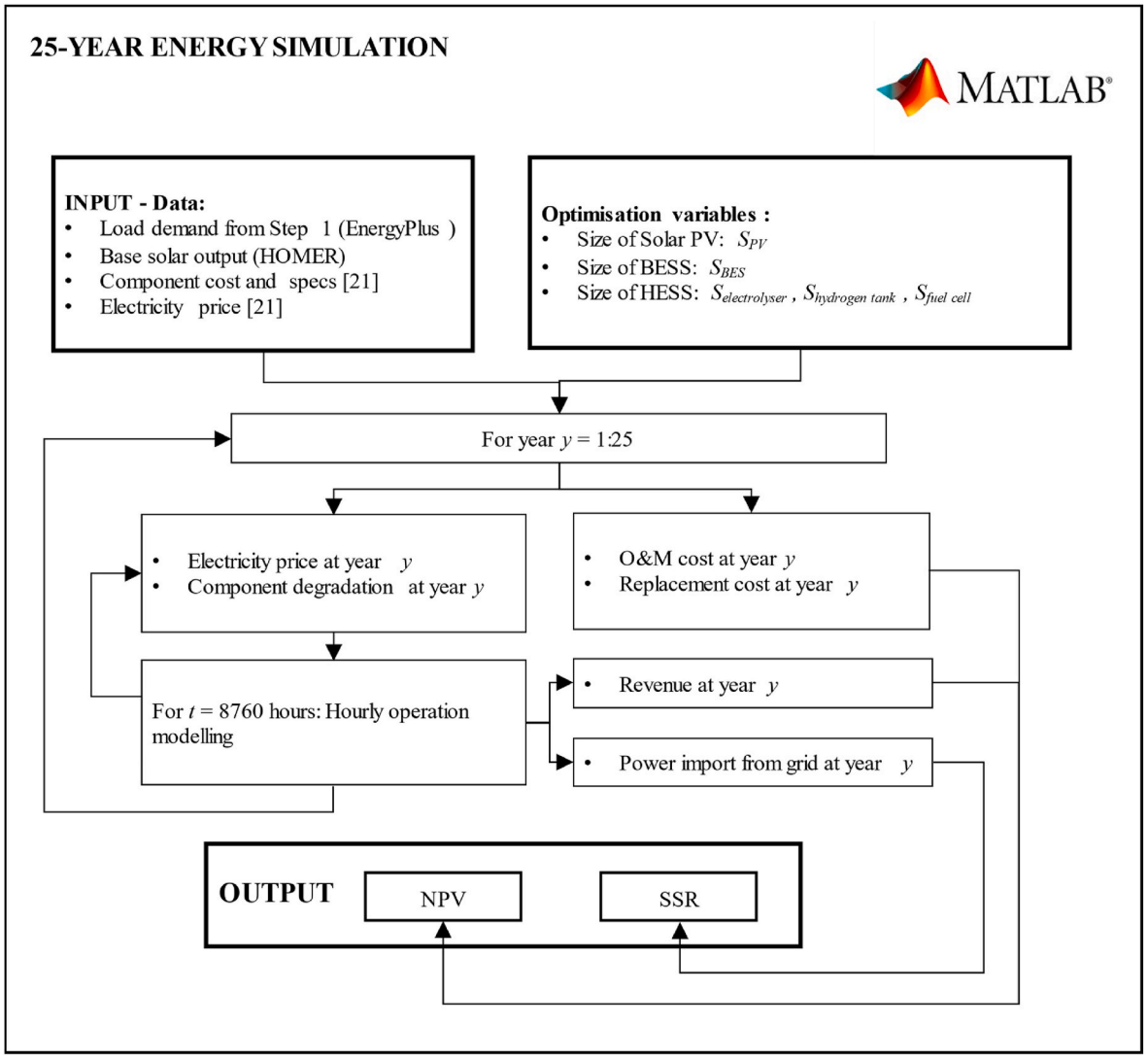

Fig. 4. The flow chart of optimisation procedure for the optimal sizing of ESSs in this study.

The optimisation process is implemented in MATLAB 2021b. The results obtained from the optimisation process, such as the size of components and total electricity imported from the grid are used as input data for the subsequent LCA analysis. For further details on the control strategy, computation of the NPV and SSR, component costs, MOMFA, and energy simulation, readers are encouraged to refer to our previous publication [21], which demonstrated the effectiveness of the proposed method from a techno-economic point of view.

2.3. Life cycle analysis

LCA is a systematic approach that encompasses several steps to assess the potential environmental impacts of a product or process (e.g., the energy consumption and RES system in the building). The goal of LCA is to identify and quantify all inputs and outputs, including emissions, and evaluate the potential environmental impacts associated with the production and use of the product. LCA typically involves four steps [50–52].

1. Goal and scope definition: specifying the product, identifying data sources, defining system boundaries, and determining the functional unit. The functional unit serves as a reference to which all the inputs and outputs are related.
2. Life Cycle Inventory (LCI): collecting data and quantifying inputs and outputs, such as raw materials, resources, energy, waste, and emissions.
3. Life Cycle Impact Assessment: determining the potential environmental impacts of the inputs and outputs identified in the LCI stage. This involves categorising and aggregating environmental interventions into impact categories, such as global warming. Characterisation factors are then calculated to determine the contribution of different substances to each impact category.
4. Interpretation: combining the findings from the inventory analysis and impact assessment to draw conclusions or make recommendations.

The LCA discussed in this paper is based on the technical guidance provided by ISO 14040 [50] and ISO 14044 [53]. ISO 14040 defines the fundamental principles and framework for conducting an LCA, while ISO 14044 outlines the requirements and guidelines for executing an LCA study.

2.3.1. Goal and scope definition

Following the optimal techno-economic analysis of the RES system for the building presented in Section 2.1 and 2.2., the goal of this LCA study is to conduct a comparative assessment of the environmental impacts of optimised systems. This analysis aims to investigate the holistic environmental impact of the optimised RES system and particularly, quantify the compensatory impacts of the size of components for the self-sufficiency building, such as PV panels, battery, electrolyser, and fuel cells.

The functional unit selected for this study is 1 kW h of electricity supplied to the building. SimaPro 9.3 [54] is employed to perform the LCA. Fig. 5 illustrates the system boundary of this study, which covers the life cycle of the system from the extraction of raw materials through the manufacturing, transportation, and use phases. The replacement of components is considered, assuming a lifespan of 5 years for the fuel cell, 15 years for the electrolyser, and 12 years for the battery. It is worth noting that the End-of-Life (EOL) phase is excluded in this study. The exclusion of the End-of-Life (EOL) phase from the analysis is based on several factors. Firstly, the EOL phase is characterized by a high degree of uncertainty, particularly within the context of microgrids, where future disposal and recycling methods of components can exhibit considerable variability. For example, when comparing an incineration and a recycling process for the PEMFC, recycling scenario results in a reduction of more than 30 % of the global warming potential category and more than 60 % in the other impact categories over the whole life-cycle [55]. Furthermore, the exclusion of the EOL phase serves as a precautionary measure because some components of the renewable scenario can potentially be reused or recycled [22]. Stropnik et al. [56] demonstrate that the different level of reused, recycled materials and landfilling in PEMFCs can yield significant reductions in environmental

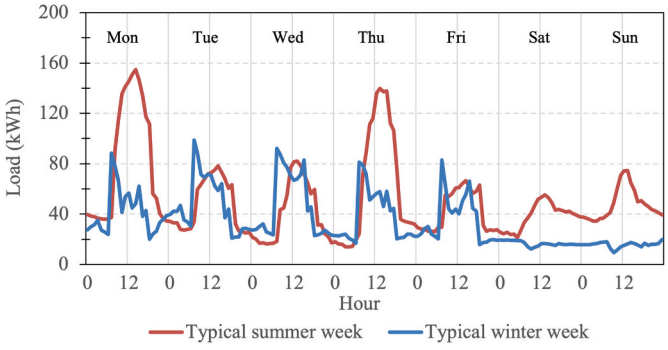

Fig. 6. Energy consumption of the office model.

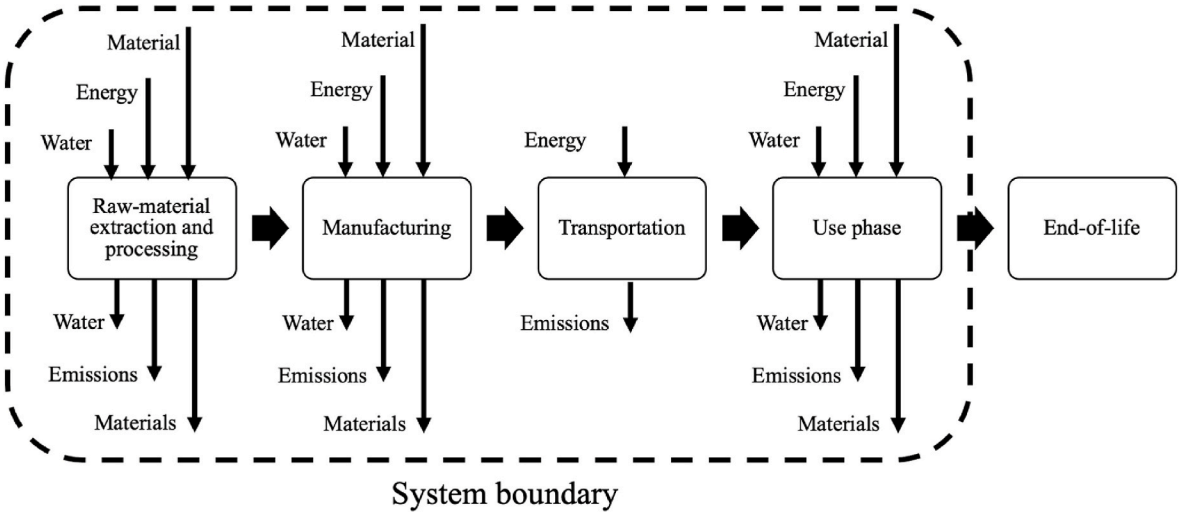

Fig. 5. System boundary for the LCA of this study.

impact indicators up to 66 %. Lastly, the recycling process itself demands energy, and the geographical location with varying electricity grid mixes can also introduce variations in the results, as demonstrated in studies [24,56]. Similar studies in the literature have also often omitted the EOL phase from their analyses [57]. Therefore, while acknowledging the importance of the EOL phase in a comprehensive LCA, this study does not include the EOL phase to simplify the analysis and maintain a focus on the primary objective of the study.

2.3.2. Life cycle inventory

The LCI involves a systematic inventory of the input and output material and energy flows throughout the system boundary. Collecting data on the production of different components from manufacturers is challenging. Therefore, to obtain the required data for input and output flows, Ecoinvent 3.8 database [58] is used, which provides comprehensive international industrial and commercial data on material production, transportation, energy consumption, and other relevant factors [58,59].

Table 2 lists the assumptions of inventories and proxy datasets used. As specific data for Australia were unavailable, the geography of all proxy datasets is set to global. The global dataset represents the average global production, which is typically based on international data. If data for the average global production are not available, the global dataset is usually generated as a weighted average of multiple local datasets or extrapolated by copying a local dataset. In such cases, the uncertainty information of the extrapolated datasets is adjusted accordingly [60]. Due to the lack of information on the exact components of the electrolyser, the fuel cell proxy dataset is used as a substitute, which is a common practice in similar studies [22,23]. To adjust for the difference between the fuel cell and the electrolyser, a scaling factor of 0.470 is applied to the electrolyser quantity. This factor is based on a study by Bionaz et al. [13], which reported GHG emissions of 190.5 kg CO_2 eq per kW installed for the electrolyser and 405.5 kg CO_2 eq per kW installed for the fuel cell. Furthermore, as the LCI can be affected by different electricity grid mixes, a sensitivity analysis considering different electricity grid mixes is also included in this study. It should be noted that the values presented in Table 2 represent the cumulative electricity generation over the entire 25-year project lifespan, which totals 7.03×10^6 kWh (further information can be found in Section 3.1). To facilitate further analysis, all quantities are normalised by dividing them by this total electricity generation figure to establish the functional unit of 1 kW h.

2.3.3. Life Cycle Impact Assessment

The LCIA is the third stage of LCA analysis, which converts the resources and emissions identified in the LCI into different environmental impact categories. The LCIA consists of two mandatory components: classification and characterisation. The classification process involves assigning emissions to appropriate impact categories, whereas most elementary flows can be assigned to a single impact category. However, some emissions cannot be attributed to a single category, and in such cases, they are assigned to all the impact categories that they affect. The characterisation is the definition of the magnitude of the impact of emissions concerning a reference substance of an impact category, which is quantified using a characterisation factor [50].

In this study, 12 potential environmental impacts are evaluated using the Environmental Footprint (EF) 3.0 method. The selected impact categories are Climate Change, Ozone Depletion, Photochemical Ozone Formation, Particulate Matter, Acidification, Freshwater Eutrophication, Terrestrial Eutrophication, Marine Eutrophication, Freshwater Ecotoxicity, Water Use, Resource Use - fossils, Resource Use - minerals and metals, which are the most relevant aspects for analysing RES [22].

Table 2
System components and approximations considered in this LCA.

	Quantity for entire lifetime[a]	Proxy dataset in Ecoinvent 3.8	Inventory assumption	Ref
Modules				
Electricity grid (kWh)	$\sum_{t=0}^{t=N} P^t_{G,imp}$	Electricity, low voltage (GLO)| market for | APOS, S	A sensitivity analysis with different grid mixes is presented in section 3.3.	
Photovoltaic (m^2)	$S_{PV}\times$ PV footprint	Photovoltaic panel, single-Si wafer (GLO) market for | APOS, S	PV footprint: 5.42 m^2/ kWp	[22]
Battery (kg)	$S_{BESS}\times$ Energy density	Battery, Li-ion, NCA, rechargeable, prismatic (GLO)| market for | APOS, S	Energy density: 150 W h/kg	[22]
Fuel cell (p)	$\frac{S_{fuel\ cell}}{2kW}$	Fuel cell, stack polymer electrolyte membrane, 2 kW electrical, future (GLO)| market for | Cut-off, S	None	[22]
Electrolyser (p)	$\frac{S_{electrolyser}}{2kW}$	Modified from: Fuel cell, stack polymer electrolyte membrane, 2 kW electrical, future (GLO)| market for | Cut-off, S	The dataset was modified by using a factor of 0.470 to the output amount of fuel cell data set.	[13, 61, 62]
Storage tank (kg)	$\frac{S_{hydrogen\ tank}}{Cm}$	Steel, chromium steel 18/8 (GLO)| market for | APOS, S	*Cm* (mass of H2 stored divided by the mass of the vessel): 0.32 %	[22]
Auxiliary components for PV system				
Mounting system (m^2)	$S_{PV}\times$ PV footprint	Photovoltaic mounting system, for 570 kWp open ground module (GLO) | market for | APOS, S	PV footprint: 5.42 m^2/ kWp	[22]
Auxiliary components for hydrogen system				
Water tank (kg)	$\frac{S_{electrolyser}}{3kW}\times 6kg$	Polyethylene terephthalate, granulate, bottle grade (GLO) | market for | APOS, S	Water tank (80 l - 6 kg) for 3 kW electrolyser	[23]
Connection cables (m)	$\frac{S_{electrolyser}+S_{fuell\ cell}}{3kW}\times 145m$	Cable, connector for computer, without plugs (GLO) | market for | APOS, S	145 m cable long for 3 kW system	[23]
Li-ion batteries (kg)	$\frac{S_{electrolyser}+S_{fuell\ cell}}{3kW}\times 145m$	Battery, Li-ion, NCA, rechargeable, prismatic (GLO)| market for | APOS, S	3.6 kW h li-ion battery for starting up 3 kW system. Energy density of	[23]

(*continued on next page*)

Table 2 (*continued*)

	Quantity for entire lifetime[a]	Proxy dataset in Ecoinvent 3.8	Inventory assumption	Ref
			battery: 150 W h/kg	
Valves, pressure regulators, pressure transmitter (kg)	$\frac{S_{electrolyser}+S_{fuell\ cell}}{3kW}\times 0.6kg$	Brass (GLO) | market for | APOS, S	0.6 kg of brass for 3 kW system	[23]
	$\frac{S_{electrolyser}+S_{fuell\ cell}}{3kW}\times 1.1kg$	Chromium steel pipe (GLO) | market for | APOS, S	1.1 kg of steel for 3 kW system	[23]
Tubing	$\frac{S_{electrolyser}+S_{fuell\ cell}}{3kW}\times 0.6kg$	Steel, chromium steel 18/8 (GLO)| market for | APOS, S	0.6 kg chromium steel pipe for 3 kW system	[23]
Auxiliary components for battery system				
Connection cables (m)	$\frac{S_{BESS}}{22kWh}\times 100m$	Cable, connector for computer, without plugs (GLO) | market for | APOS, S	100 m cable long for 22 kW h system	[23]

[a] Where $\sum_{t=0}^{t=N} P_{G,imp}^{t}$ is total power imported from the grid during the entire project life time N of 25 years, as discussed in Eq. (7); S_i is size of component *i*, which is obtained following the optimisation process illustrated in Fig. 1.

3. Result and discussion

3.1. Energy demand and RES simulation

This section presents the results of the energy demand and optimisation of the microgrid presented in Sections 2.1 and 2.2, respectively. Fig. 6 illustrates the energy consumption of the office model during a typical summer and winter week. Fig. 6 shows that the highest load demand occurs during working hours. Melbourne experiences highly unpredictable weather patterns, with occasional exceptionally hot days during the summer season, leading to increased demand for cooling and significant energy consumption, as evidenced by the spikes on Mon and Thu in Fig. 6. Conversely, the temperature remains relatively stable during the winter season, resulting in a consistent heating load during working hours. Despite the building is not in use during non-working hours, it still consumes some energy to maintain temperature setpoints.

Fig. 7 shows the optimised capacities of the PV, battery, electrolyser, hydrogen tank, and fuel cell for various SSR. As the SSR increases, the optimised capacities of all components generally increase, although this relationship is complex, particularly as the system approaches full renewable capacity. Notably, after reaching an SSR of 98.20 %, the optimal capacities of PV, battery, and hydrogen tank increase more rapidly than those of the other components. PV is the largest contributor to the system, as it not only provides direct electricity for usage but also charges the BESS and HESS. Therefore, its optimised capacity always increases as the SSR increases. The optimised capacities of the BESS and hydrogen tank also increase as the system approaches full renewable energy to meet the electric demand on exceptionally hot days, as shown in Fig. 6. On the other hand, as the system approaches full renewable capacity, the optimised capacities of the electrolyser and fuel cell do not change much, indicating that their use is primarily for peak shaving and backup purposes. It is worth noting that the size of the components may fluctuate as the optimisation algorithm employed in this study is a heuristic method that provides approximate solutions, which are efficient and accurate enough for these optimisation problems [63–65]. In addition, the interval for the SSR values is not predetermined, but rather is determined through the optimisation process. The heuristic MOMFA optimisation algorithm moves the firefly to maximise objectives, and the interval of SSR values is dependent on the randomness of the firefly movement and generation until convergence.

The building energy analysis estimated that the annual electric load is 281,479 kW h, which corresponds to approximately 7 million kWh over a 25-year period. Fig. 8 shows the load coverage breakdown from the RES systems at different SSR levels. Direct usage from PV is consistently the primary energy source, providing over half of the total energy required to meet the load demand. At most SSR levels, BESS and HESS contribute almost equally to the load, although the contribution of BESS increases more rapidly as the SSR level increases. The average contribution across all SSR levels for BESS and HESS is 21.3 % and 18.1 %, respectively. As the SSR approaches 100 %, the contribution of the grid decreases, while PV does not experience a significant increase, resulting in storage systems such as BESS and HESS becoming the predominant energy sources.

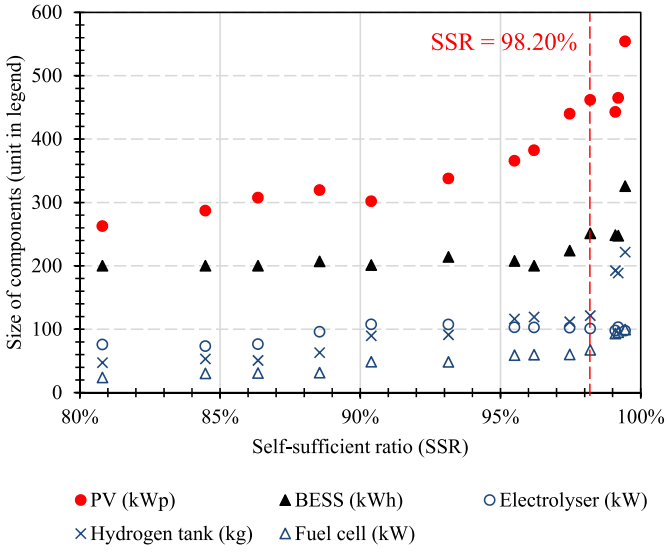

Fig. 7. Optimised PV, battery, electrolyser, hydrogen tank, and fuel cell capacity of individuals at self-sufficient ratio (SSR).

3.2. Results of the LCA

This section discusses the LCA results of the optimised RES systems presented in Fig. 7. Firstly, prior to modelling the life cycle of all systems in Section 3.1, the first system with SSR of 80.81 % is chosen to analyse the share of auxiliaries to the overall environmental impact. As depicted in Fig. 9, auxiliaries accounted for a relatively small proportion of the total impacts, ranging from 5 % to 7 % across selected categories, with the exception of 11 % in the case of particulate matter. This finding is consistent with the results from previous studies, specifically, Gandiglio

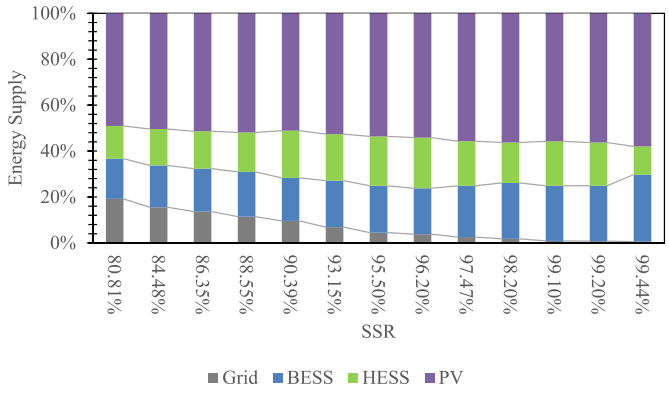

Fig. 8. Breakdown of the load coverage at different SSR.

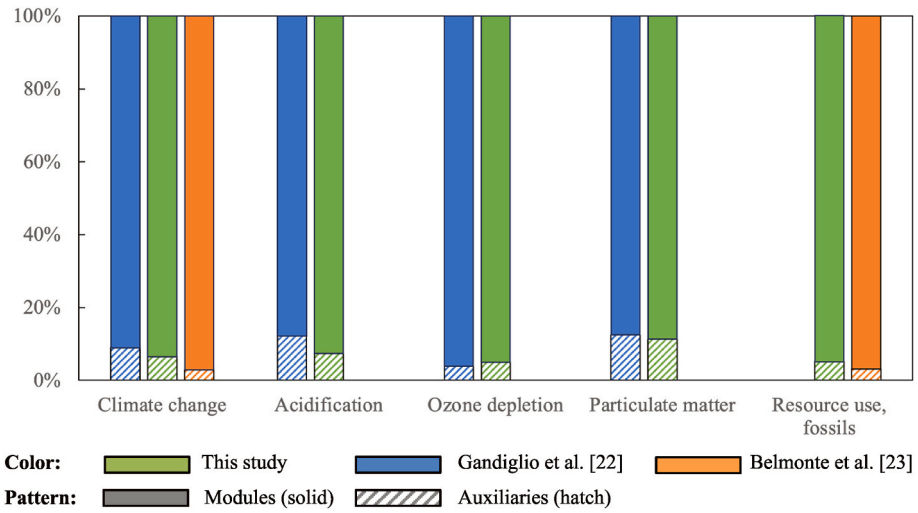

Fig. 9. Contributions of auxiliaries to selected impacts in LCA.

et al. [22] and Belmonte et al. [23]. It's noteworthy that a direct comparison with the study of Gandiglio and colleagues is feasible since the studies both employ the EF 3.0 method in LCIA. However, in the case of Belmonte et al. [23], which employs the Impact 2002+ method, crude comparison is obtained. Nevertheless, the results of our study, as well as those from the aforementioned literature, consistently indicate that the contribution of auxiliaries to environmental impacts tends to be relatively modest. Additionally, certain components of auxiliaries are site-specific. For instance, cable length depends on the location of the system to the point of connection. Consequently, while auxiliaries might represent essential components in a comprehensive LCA, only modules are modelled for all 15 microgrids in this study (Step 3 of the framework in Fig. 1). This approach simplifies the analysis while still maintaining the primary focus of this study which is to provide insights into the environmental impacts with varying SSRs and to assess the distribution of these impacts among different SSR scenarios.

In this study, the primary environmental metric is climate change impacts, measured in kilograms of carbon dioxide equivalent (kg CO_2 eq). Kg CO_2 eq is a commonly used scale for comparing different greenhouse gases and represents the amount of CO_2 emissions that would cause the same warming effect over a standard 100-year time horizon [13]. Fig. 10 presents the climate change impacts associated with 1 kW h of electricity supplied at different SSRs. Across all SSRs, the top three contributors to climate change impact are carbon dioxide (average of 87.21 %), methane (average of 9.45 %), and dinitrogen monoxide (average of 1.06 %). The results indicate that the highest impact of 0.22 kg CO_2 eq/kWh is observed at the lowest SSR of 80.81 %. As SSR increases to 96.20 %, the climate change impact decreases to its lowest value of 0.15 kg CO_2 eq/kWh. However, as the SSR continues increasing (i.e., the building approaches self-sufficiency) the impact significantly increases reaching 0.19 kg CO_2 eq/kWh at the SSR of 99.44 % as shown in Fig. 10. The trend observed in Fig. 10 is consistent with the results presented in Fig. 7, which indicates that there exists an optimal threshold of SSR. Beyond this threshold, a rapid increase in the size of the components is observed, leading to a higher carbon footprint. It should be noted that the exclusion of auxiliaries may potentially lead to an underestimation of the climate change impact, particularly for systems characterized by very high SSRs. This is due to the possibility that the proportion of auxiliaries, and thus their associated environmental impact, could increase during the transition towards RES-dominant systems. However, this acknowledgment of potential uncertainties should not diminish the significance of the trends observed in Fig. 10. Also, as discussed in Section 2.3.1, the exclusion of EoL may introduces certain uncertainties. However, previous studies [24,66] have indicated that the EoL phase typically makes a negligible contribution to the environmental impacts of the system, though in certain cases, it can account for up to 10 % of the climate change impact due to the recovery of some materials [66]. To analyse the detailed impacts of each component, three systems were selected for further analysis, including the lowest SSR of 80.81 %, the SSR with the lowest impact of 96.20 %, and the highest SSR of 99.44 %.

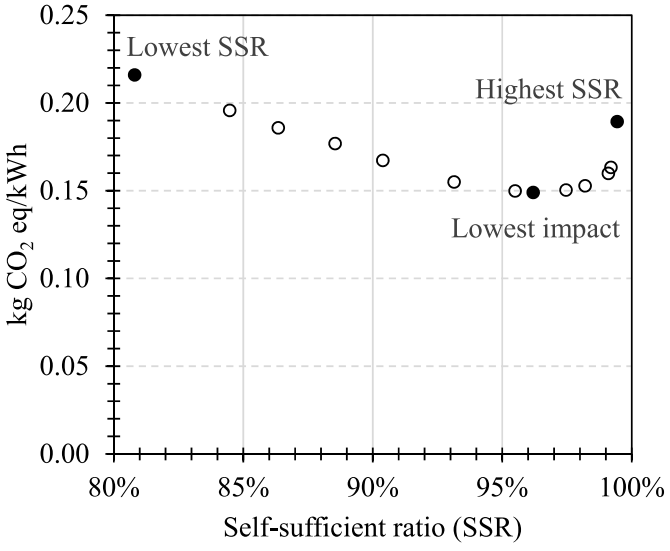

Fig. 10. Climate change impacts associated with 1 kW h of electricity supplied at different self-sufficient ratio (SSR).

Fig. 11 compares all the environmental impact of three selected scenarios. The scores in each category are normalised relative to the highest score, which is scaled to 100 %. The results reveal that at the case of SSR of 96.20 %, which has the lowest climate change impact as presented in Fig. 10, also has the lowest impacts in many other categories. It is interesting to observe in Fig. 11 that the case of SSR of 99.44 % (i.e., nearly 100 % of energy consumption is provided by PV and ESS) is dominant in most of impact categories (9 over 12). This includes the categories of ozone depletion, particulate matter, acidification, eutrophication in all categories, and resource use for fossils, minerals, and metals. This result indicates that achieving very high self-sufficiency ratios may require significant resource inputs, which can offset the benefits of renewable energy in many impact categories. Finally, for the case of SSR of 80.81 %, the impacts are the highest in some categories

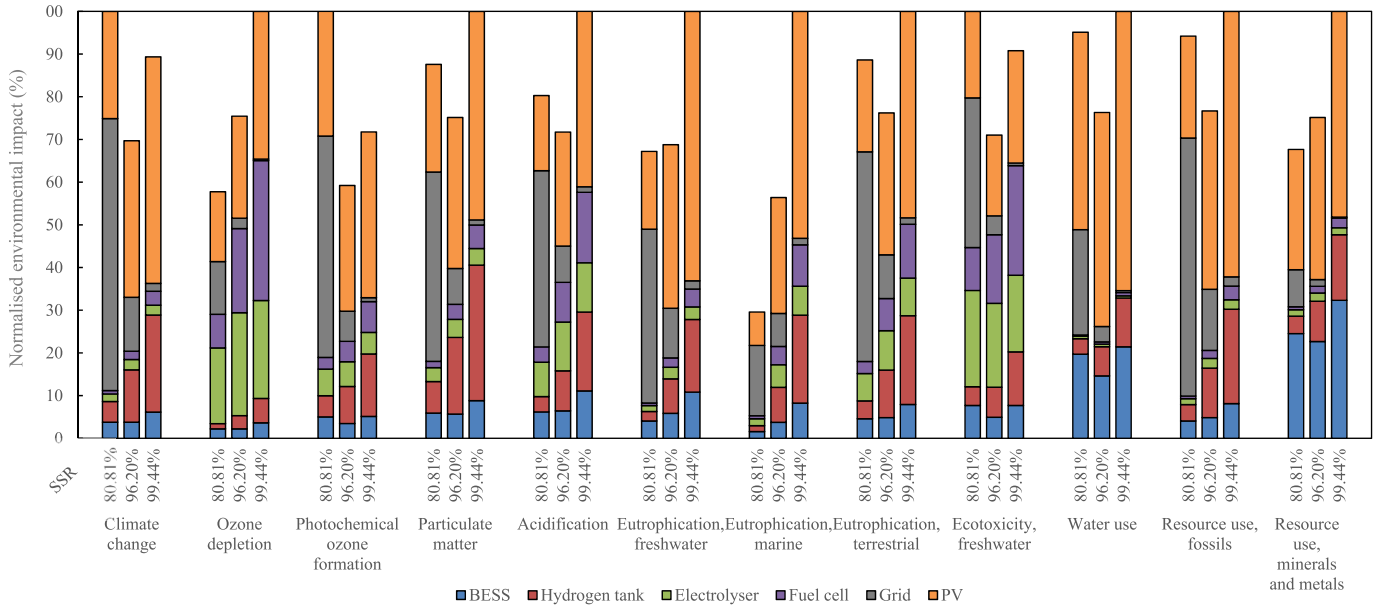

Fig. 11. Breakdown of the impacts of the selected SSR.

such as climate change, photochemical ozone formation, and ecotoxicity in freshwater. Overall, the results from Fig. 11 highlight the importance of considering a broad set of impact categories when assessing the sustainability of self-sufficient buildings powered by RESs. Although achieving a very high SSR of 99.44 % can lead to lower environmental impacts in the climate change category compared to an SSR of 80.81 %, as indicated in Figs. 10 and 11, the trade-offs between impact categories should be carefully considered. This is particularly important given the dominance of the case of SSR of 99.44 % in most impact categories, which substantial inputs of raw materials, energy, and water resources that can offset the benefits of renewable energy.

Furthermore, Fig. 11 reveals two distinct patterns. Firstly, most of the environmental impacts follow a similar trend to that of climate change impacts in Fig. 10, with a reduction to a minimum of 96.20 % SSR followed by an increase. Secondly, for four impact categories, namely ozone depletion, eutrophication in freshwater and marine, and resource use of minerals and metals, higher SSR levels result in higher impacts. In terms of ozone depletion, this impact category calculates the destructive effects on the stratospheric ozone layer over a time horizon of 100 years. This category is one of very few impact categories that electrolyser and fuel cell have a noticeable contribution. According to the inventory analysis, tetrafluoroethylene is a major contributor to the ozone depletion potential of fuel cell stacks, accounting for 98 % of the total impact. Tetrafluoroethylene is used in the production of polymer polytetrafluoroethylene, which is copolymerised with a perfluorosulfonic acid polymer membrane used as an electrolyte in proton exchange membrane fuel cells (PEMFC). Despite its use in PEMFC, the significant impact of tetrafluoroethylene on ozone depletion highlights the need for further research and development of alternative materials in fuel cell stack production. The impact indicators for eutrophication in freshwater and marine environments are expressed in terms of phosphorus and nitrogen equivalents, respectively. Eutrophication freshwater measures the degree to which emitted nutrients reach the freshwater end compartment, while eutrophication marine measures the degree to which emitted nutrients reach the marine end compartment. The production of silicon in PV panels is the primary contributor to the high impact of eutrophication in freshwater and marine environments. Resource use - minerals and metals is focused on the depletion of non-renewable resources such as metals and minerals. Thus, the component sizes of the RES directly translate into the resource use - minerals and metals category. Specifically, in Fig. 7, when comparing two micro-grid with SSRs of 80.81 % and 96.20 %, only the sizes of the PV panels and hydrogen tank increase, leading to a higher minerals and metals resource use in Fig. 11, while the BESS size slightly reduces, resulting in a decrease in this category. When the SSR increases to 99.44 %, the rapid increase in the sizes of all components (PV panels, hydrogen tank, and battery) will significantly increase resource use - minerals and metals.

Furthermore, from Fig. 11, it is also evident that PV systems and grid contribute to a large portion of impacts in many categories. For PV systems, this is mainly due to the production process of silicon, which requires a significant amount of energy for its purity process [23]. In addition, the processing and manufacturing of PV also contribute significantly to emissions of criteria pollutants such as SO_2, NO_x [67] and these pollutants can lead to particulate matter formation and photochemical oxidation [68]. However, it is important to note that the high impact of PV systems on various environmental categories is due to their enormous size, which is necessary to generate excess electricity for charging the battery and hydrogen energy storage system. Additionally, the PV system must account for losses in the renewable energy system, such as the low efficiency of the hydrogen generators and fuel cells (Power-to-Gas-to-Power). As a result, the environmental impacts associated with the production and operation of PV systems are not solely due to their inherent processing and manufacturing but also reflect the energy inputs required to support other components in the RES. For the electricity grid, the global electricity grid dataset is a representative mix in the global geography, with major contributions from Asia (47 %), Northern America (22 %), and Europe (15 %). As highlighted in Section 3.3, global electricity production still relies heavily on fossil fuels. This reliance results in the disposal of coal ash (hard coal and lignite) from thermal power plants and spoils from coal mining, which are the main sources of ecotoxicity in freshwater [69].

Fig. 12 focus on the contribution of ESSs in the climate change impact of the three selected systems. At the lowest SSR of 80.81 %, the ESS accounts for only 9 % of the total climate change impact, while the grid is the largest contributor at 65 %. This is notable given that Fig. 8 shows that the grid supplies only around 20 % of the load. In contrast, PV supplies almost 50 % of the load and only contributes 26 % to the total climate change impact. As the SSR rises to 96.20 %, the impact of ESSs on climate change increases to 27 %, with PV contributing 54 % and grid contributing decreasing to 19 %. When the SSR reaches its highest value of 99.44 %, ESSs contribute to 36 % of the climate change impact, PV systems account for 62 %, and the contribution from the grid

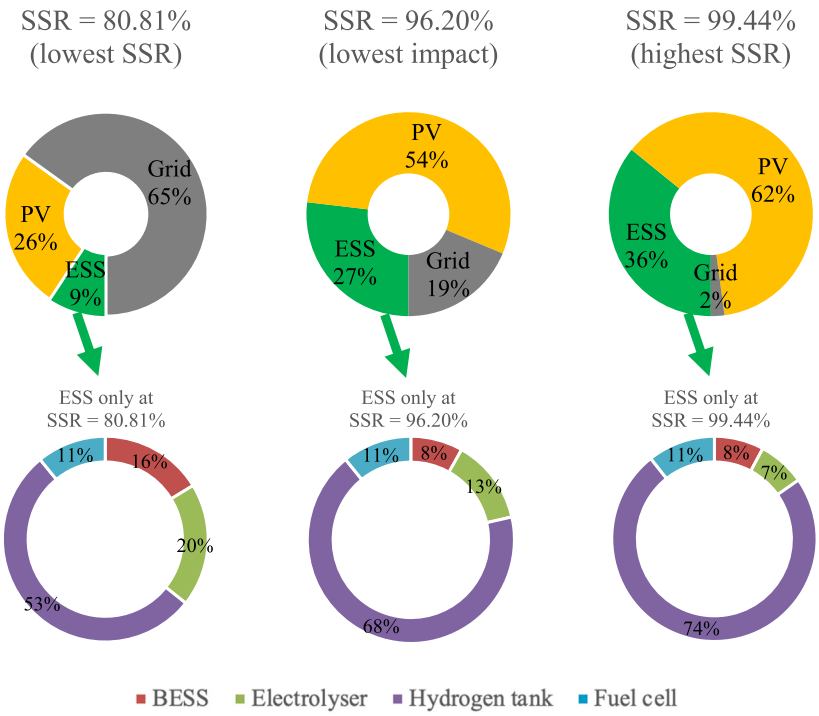

Fig. 12. Climate change impact comparison of selected SSR with focus on ESS contribution.

system drops substantially to a mere 2 %.

Fig. 12 also provides the climate change impact associated with the various components of the ESSs, including BESS, electrolyser, hydrogen tank, and fuel cell. Despite the BESS and HESS contributing almost equally to the load in Figs. 8 and 12 shows that the BESS only accounts for a small impact, ranging between 8 % and 16 % among the selected SSR. This is due to the use of nickel cobalt aluminium oxide (NCA) batteries, which are considered the most sustainable Li-ion batteries for micro-grid with PV applications. The combination of cobalt and other cathode materials in NCA batteries provides the best trade-off between high energy density, materials consumption, and lifecycle duration [27].

The climate change impact associated with the hydrogen tank in the HESS is typically the highest among the ESS components due to the substantial amount of steel required for its manufacturing. It takes about 100 kg of steel to store 1 kg of H2 [70]. The impact of steel production, which involves the production processes of ferronickel and ferrochromium, is the primary reason for its high impact. This finding is consistent with similar studies [13,23,70], which have indicated that hydrogen storage tanks often contribute significantly to the climate change impact of RESs. In addition, storage pressure and weight performance (which is the mass of H2 stored divided by the mass of the vessel) are aspect to consider on the efficiency of the storage system. This study is based on inventory data from Gandiglio et al. [22], which assumes a storage pressure of only 28 bar. This means that the result in Fig. 12 is based on a specific storage pressure scenario, and variations in pressure levels could yield different results. For instance, higher storage pressures might require a thicker steel layer but can improve weight performance. However, the pressure at which hydrogen is stored affects the energy required for compression and decompression, which, in turn, can have implications for the overall energy balance and emissions associated with the RES system. Higher storage pressures generally require more energy for compression, potentially leading to increased greenhouse gas emissions if the energy source used for compression is carbon intensive.

Despite fuel cells and electrolysers require the use of critical and transient metals, such as platinum and titanium, as well as rare-earth metals during the manufacturing phase [61], they have a minimal environmental impact. This is because only very small amounts of platinum are used in the inventory database. Furthermore, as already mentioned in Section 2.3.2, the electrolyser is approximated to a fuel cell using a scaling factor. However, it is recommended to use specific data for the different types of electrolysers. For instance, an alkaline electrolyser requires fewer platinum group metals than a polymer electrolyte membrane electrolyser (PEMEL) [23]. In an alkaline electrolyser, only the cathode active material consists of a blend of Pt, C, and Ni, whereas the anode active material is a mixture of Ni, Co, and Fe [71]. In contrast, the only active materials used in the cathode and anode of a PEMEL are platinum and iridium, respectively [71].

3.3. Sensitivity analysis

As previously mentioned, a sensitivity analysis is conducted to assess the effect of different grid mixes on the climate change impact. Fig. 13 presents the breakdown of the global electricity production mix by source for the reference years, based on data from the IEA World Energy Balances [72]. Coal, gas, hydro, and nuclear are the primary sources of electricity globally, accounting for 87 %, while other renewables represent a smaller share. In addition to the global mix, three other mixes (A, B, C) are selected for the sensitivity analysis. Grid mix A has a much higher carbon footprint than the global mix due to its heavy reliance on coal. Grid mix B, on the other hand, relies on coal, gas, and nuclear power sources, but is less carbon-intensive than the global grid mix. Grid mix C has a high percentage of renewable energy, with 99 % of the energy sources being renewable, including hydro (52 %), nuclear (37 %), and other renewables (9 %).

Fig. 14 depicts the results of the climate change impacts of the representative countries. For scenarios where coal and gas still play a major role in electricity production, the curves have a convex shape with a decrease in climate change impact to a minimum value of approximately 95 %–98 % as SSR increases. As shown in Fig. 13, electricity mix in grid mix A is dominated by coal. Consequently, the sensitivity analysis presented in Fig. 14 shows a steeper slope of the convex curve,

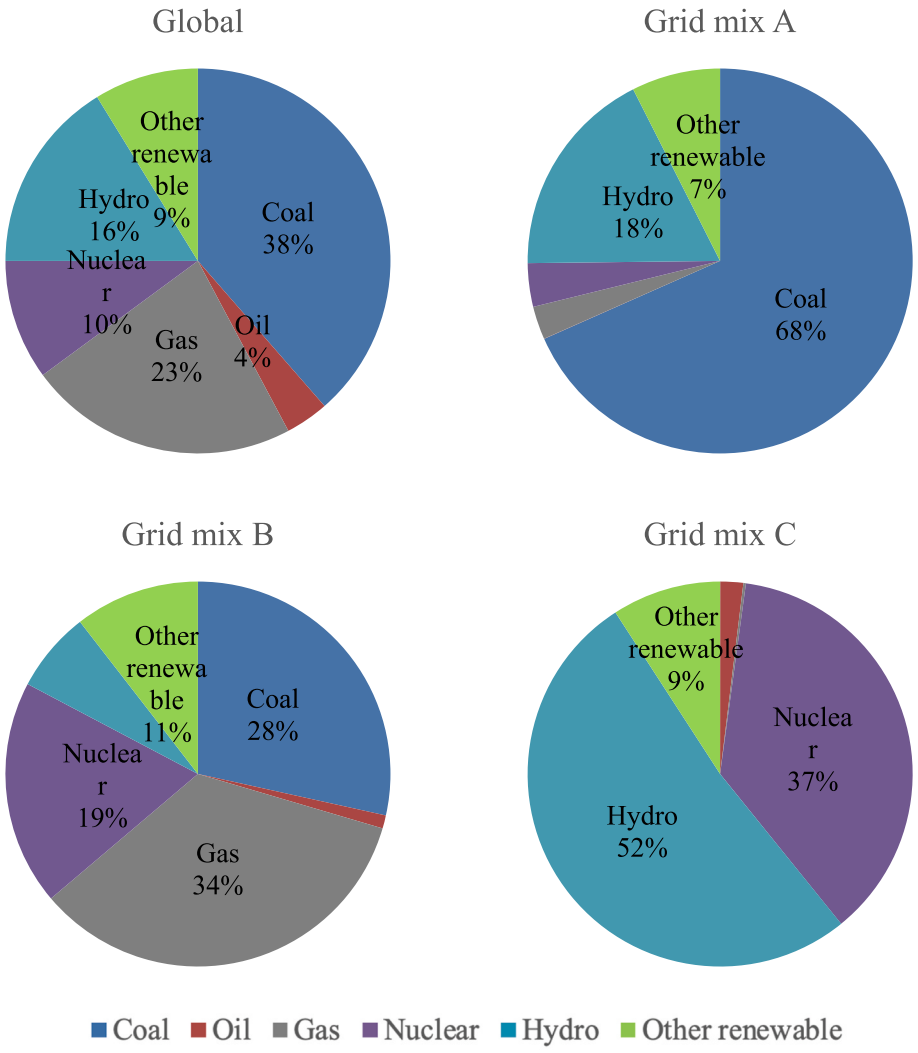

Fig. 13. Proportions of electricity production mix by the source based on data from IEA [72].

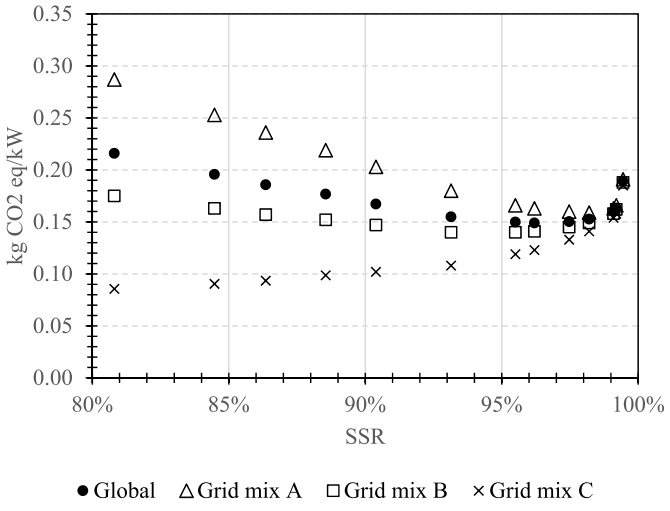

Fig. 14. Sensitivity analysis of climate change impacts associated with different electricity mix.

indicating the high potential to reduce climate change impacts by approximately 50 % from 0.29 kg CO_2 eq/kW to 0.16 kg CO_2 eq/kW at very high renewable penetration. The grid mix B has a less carbon-intensive electricity grid than the global average, but still relies heavily on coal and gas, resulting in a convex slope that is less steep than the global curve. In contrast, grid mix C sources almost all of its energy from renewable sources, which corresponds to the observation that a higher SSR that does not translate to a lower climate change impact but rather exacerbates it. This indicates that focusing on fully renewable energy in buildings in locations such as grid mix C is undesirable because of the country's existing renewable energy sources from the grid. Setting up a large RES within buildings requires more resources and cannot leverage economies of scale. This emphasizes the importance of coexisting decentralised RESs in zero future buildings with a centralised large-scale renewable energy production.

4. Conclusion

In conclusion, this study investigates the environmental impacts of microgrids with varying SSRs for a three-floor office building. While LCA has been widely used to evaluate the environmental impacts of energy storage systems for buildings and residential applications, most previous studies have only examined single configurations under a specific SSR, which were pre-optimised or designed. On the other hand, this study uses optimisation modelling to determine the optimal capacity and breakdown of the load coverage for a set of different SSRs. The study then conducts multiple LCAs under various scenarios, each with different optimised component capacities and load coverage.

The optimisation results indicate that as the SSR increases, the optimised capacities of all components generally increase. PV, battery, and hydrogen tank capacities increase more rapidly than other components as the system approached full renewable capacity. Direct usage from PV is the primary energy source, accounting for more than half of the energy required to meet the load demand. BESS and HESS usually contribute equally to the load, with contribution from BESS increasing more rapidly as SSR increases. The LCA reveals that as the SSR increases, the climate change impact decreases; however, as the SSR approaches fully renewable levels (approaching 100 %), the impact increases again due to the rapid growth in component sizes. It is important to consider a broad set of impact categories to have a comprehensive environmental impacts assessment. For instance, although the highest SSR does not translate to the highest climate change impact, it still dominates in 9 out 11 other impact categories. Finally, the sensitivity analysis presents the potential impact of different grid mixes on the overall climate change impact. Countries with a carbon-intensive electricity grid can reduce the impact of climate change by increasing their SSR to a very high renewable penetration. On the other hand, countries with a high proportion of energy from renewable sources may not see a decrease in climate change impact by relying on decentralised renewable energy sources within buildings and should instead focus on coexisting decentralised and centralised large-scale renewable energy production.

While this study provides valuable insights into the environmental impacts of different renewable energy systems at different SSR, future studies could explore additional aspects. This study only considers electricity demand for heating and cooling. Future investigations could benefit from an expanded scope to include state of arts technologies such as thermal energy storage systems and heat pumps. Additionally, this study assumes constant data over the system lifetime and does not consider uncertainties associated with demand profiles and input data. However, acknowledging the uncertainties inherent in LCA, such as weather conditions and performance efficiency, is an essential topic in future research. Finally, while this study provides a foundational perspective, the absence of full LCAs that includes EoL phases, along with different disposal and recycling methods, highlight the importance for continuing research. Considering the substantial number of renewable systems already in operation and their projected expansion, the proper disposal of these systems, the disposal of these system is expected to become an environmental issue in the next decades. Thus, future efforts should emphasize gaining comprehensive understanding of the processes involved in the conclusion of the operational life of renewable energy system.

CRediT authorship contribution statement

Son Tay Le: Methodology, Investigation, Software, Visualization, Writing - original draft. **Tuan Ngoc Nguyen:** Methodology, Investigation, Software, Supervision, Writing - review & editing. **Dac-Khuong Bui:** Methodology, Software. **Birch Teodosio:** Supervision, Writing - review & editing. **Tuan Duc Ngo:** Conceptualization, Supervision, Writing - review & editing.

Declaration of competing interest

The authors declare that they have no known competing financial interests or personal relationships that could have appeared to influence the work reported in this paper.

Data availability

The authors are unable or have chosen not to specify which data has been used.

Acknowledgment

This research was supported by the Melbourne Postdoctoral Fellowship and the ARC Linkage Project (ARC LP210200774). The first author, Tay Son Le, would like to thank the University of Melbourne for offering the Melbourne Research Scholarship.

References

[1] United Nations Environment Programme. 2020 global status report for buildings and construction: towards a zero-emission, efficient and resilient buildings and construction sector. 2020. Nairobi.
[2] Robledo CB, et al. Integrating a hydrogen fuel cell electric vehicle with vehicle-to-grid technology, photovoltaic power and a residential building. Appl Energy 2018;215:615–29.
[3] Izadi A, Shahafve M, Ahmadi P. Neural network genetic algorithm optimization of a transient hybrid renewable energy system with solar/wind and hydrogen storage system for zero energy buildings at various climate conditions. Energy Convers Manag 2022;260:115593.
[4] Zhang L, Harnefors L, Nee H-P. Power-synchronization control of grid-connected voltage-source converters. IEEE Trans Power Syst 2009;25(2):809–20.
[5] Tang H, Wang S. Life-cycle economic analysis of thermal energy storage, new and second-life batteries in buildings for providing multiple flexibility services in electricity markets. Energy 2023;264:126270.
[6] Stougie L, et al. Multi-dimensional life cycle assessment of decentralised energy storage systems. Energy 2019;182:535–43.
[7] Liu Z, et al. A novel distributed energy system combining hybrid energy storage and a multi-objective optimization method for nearly zero-energy communities and buildings. Energy 2022;239:122577.
[8] Chauhan A, Saini R. A review on Integrated Renewable Energy System based power generation for stand-alone applications: configurations, storage options, sizing methodologies and control. Renew Sustain Energy Rev 2014;38:99–120.
[9] Hajiaghasi S, Salemnia A, Hamzeh M. Hybrid energy storage system for microgrids applications: a review. J Energy Storage 2019;21:543–70.
[10] Eriksson E, Gray EM. Optimization and integration of hybrid renewable energy hydrogen fuel cell energy systems–A critical review. Appl Energy 2017;202:348–64.
[11] Li C, et al. Exploring the interaction between renewables and energy storage for zero-carbon electricity systems. Energy 2022;261:125247.
[12] Elberry AM, et al. Large-scale compressed hydrogen storage as part of renewable electricity storage systems. Int J Hydrogen Energy 2021;46(29):15671–90.
[13] Bionaz D, et al. Life cycle environmental analysis of a hydrogen-based energy storage system for remote applications. Energy Rep 2022;8:5080–92.
[14] Buffo G, et al. Power-to-X and power-to-power routes. In: Solar hydrogen production. Elsevier; 2019. p. 529–57.
[15] Gabrielli P, et al. Optimal design of multi-energy systems with seasonal storage. Appl Energy 2018;219:408–24.
[16] Zhang Y, et al. Comparative study of hydrogen storage and battery storage in grid connected photovoltaic system: storage sizing and rule-based operation. Appl Energy 2017;201:397–411.
[17] Ren H, et al. Optimal operation of a grid-connected hybrid PV/fuel cell/battery energy system for residential applications. Energy 2016;113:702–12.
[18] Chadly A, et al. Techno-economic analysis of energy storage systems using reversible fuel cells and rechargeable batteries in green buildings. Energy 2022;247:123466.
[19] Tahani M, Babayan N, Pouyaei A. Optimization of PV/Wind/Battery stand-alone system, using hybrid FPA/SA algorithm and CFD simulation, case study: Tehran. Energy Convers Manag 2015;106:644–59.
[20] Gabrielli P, et al. Robust and optimal design of multi-energy systems with seasonal storage through uncertainty analysis. Appl Energy 2019;238:1192–210.
[21] Le TS, et al. Optimal sizing of renewable energy storage: a techno-economic analysis of hydrogen, battery and hybrid systems considering degradation and seasonal storage. Appl Energy 2023;336:120817.
[22] Gandiglio M, et al. Life cycle assessment of a renewable energy system with hydrogen-battery storage for a remote off-grid community. Int J Hydrogen Energy 2022;47(77):32822–34.
[23] Belmonte N, et al. A comparison of energy storage from renewable sources through batteries and fuel cells: a case study in Turin, Italy. Int J Hydrogen Energy 2016;41(46):21427–38.
[24] Mendecka B, Tribioli L, Cozzolino R. Life Cycle Assessment of a stand-alone solar-based polygeneration power plant for a commercial building in different climate zones. Renew Energy 2020;154:1132–43.
[25] Peppas A, et al. Performance evaluation and life cycle analysis of RES-hydrogen hybrid energy system for office building. Int J Hydrogen Energy 2021;46(9):6286–98.
[26] Di Florio G, et al. Comparative life cycle assessment of two different SOFC-based cogeneration systems with thermal energy storage integrated into a single-family house nanogrid. Appl Energy 2021;285:116378.
[27] Rossi F, et al. Environmental analysis of a nano-grid: a life cycle assessment. Sci Total Environ 2020;700:134814.
[28] DOE, U.S. Commercial reference buildings. Available from: https://www.energy.gov/.

[29] Bui D-K, et al. Biomimetic adaptive electrochromic windows for enhancing building energy efficiency. Appl Energy 2021;300:117341.
[30] Hart M, De Dear R. Weather sensitivity in household appliance energy end-use. Energy Build 2004;36(2):161–74.
[31] Lam JC, et al. Multiple regression models for energy use in air-conditioned office buildings in different climates. Energy Convers Manag 2010;51(12):2692–7.
[32] Zhang Y, et al. Battery sizing and rule-based operation of grid-connected photovoltaic-battery system: a case study in Sweden. Energy Convers Manag 2017;133:249–63.
[33] HOMER PRO. USA: HOMER energy. 2022.
[34] HOMER PRO. HOMER pro 3.14 user manual. Available from: https://www.homerenergy.com/products/pro/docs/latest/index.html; 2020.
[35] Moghaddam MJH, et al. Optimal sizing and energy management of stand-alone hybrid photovoltaic/wind system based on hydrogen storage considering LOEE and LOLE reliability indices using flower pollination algorithm. Renew Energy 2019;135:1412–34.
[36] Dong W, Li Y, Xiang J. Optimal sizing of a stand-alone hybrid power system based on battery/hydrogen with an improved ant colony optimization. Energies 2016;9(10):785.
[37] Sanajaoba S. Optimal sizing of off-grid hybrid energy system based on minimum cost of energy and reliability criteria using firefly algorithm. Sol Energy 2019;188:655–66.
[38] Maleki A, Pourfayaz F. Sizing of stand-alone photovoltaic/wind/diesel system with battery and fuel cell storage devices by harmony search algorithm. J Energy Storage 2015;2:30–42.
[39] Notton G, Lazarov V, Stoyanov L. Optimal sizing of a grid-connected PV system for various PV module technologies and inclinations, inverter efficiency characteristics and locations. Renew Energy 2010;35(2):541–54.
[40] Renewables ITP. Public report 11: lithium-ion battery testing. IT Power (Australia) Pty Ltd; 2021.
[41] Zhang W, et al. Sizing a stand-alone solar-wind-hydrogen energy system using weather forecasting and a hybrid search optimization algorithm. Energy Convers Manag 2019;180:609–21.
[42] Birol F. The future of hydrogen: seizing today's opportunities. 2019. Report prepared by the IEA for the G20, 82-83, Japan.
[43] DOE, U.S. DOE technical Targets for hydrogen delivery. Available from: https://www.energy.gov/eere/fuelcells/doe-technical-targets-hydrogen-delivery; 2022.
[44] RTIC. Energy storage grand challenge roadmap. U.S. Department of Energy's Research Technology Investment Committee (RTIC); 2020.
[45] Yang X-S. Firefly algorithms for multimodal optimization. In: International symposium on stochastic algorithms. Springer; 2009.
[46] Chou J-S, Ngo N-T. Modified firefly algorithm for multidimensional optimization in structural design problems. Struct Multidiscip Optim 2017;55(6):2013–28.
[47] Bui D-K, et al. An artificial neural network (ANN) expert system enhanced with the electromagnetism-based firefly algorithm (EFA) for predicting the energy consumption in buildings. Energy 2020;190:116370.
[48] Bui D-K, et al. Enhancing building energy efficiency by adaptive façade: a computational optimization approach. Appl Energy 2020;265:114797.
[49] Bui D-K, et al. A modified firefly algorithm-artificial neural network expert system for predicting compressive and tensile strength of high-performance concrete. Construct Build Mater 2018;180:320–33.
[50] (ISO), I.S.O., ISO 14040:2006. Environmental management – life cycle assessment – principles and framework. 2006.
[51] Hollerud B, et al. A review of life cycle assessment tools. Minneapolis, USA: Dovetail Partners Inc.; 2017.
[52] Su X, et al. Life cycle assessment of three typical solar energy utilization systems in different regions of China. Energy 2023;278:127736.
[53] (ISO), I.S.O. ISO 14044:2006 Environmental management — life cycle assessment — requirements and guidelines. 2006.
[54] SimaPro. The world's leading LCA software. Available from: https://simapro.com; 2023.
[55] Duclos L, et al. Environmental assessment of proton exchange membrane fuel cell platinum catalyst recycling. J Clean Prod 2017;142:2618–28.
[56] Stropnik R, et al. Reducing environmental impacts of the ups system based on PEM fuel cell with circular economy. Energy 2018;165:824–35.
[57] Latunussa CE, et al. Life Cycle Assessment of an innovative recycling process for crystalline silicon photovoltaic panels. Sol Energy Mater Sol Cell 2016;156:101–11.
[58] Ecoinvent. *ecoinvent v3.8 Database*. Available from: https://ecoinvent.org/the-ecoinvent-database/data-releases/ecoinvent-3-8/; 2023.
[59] Mahmud MP, et al. Environmental impacts of solar-photovoltaic and solar-thermal systems with life-cycle assessment. Energies 2018;11(9):2346.
[60] Ecoinvent. *Database geographies*. Available from: https://ecoinvent.org/the-ecoinvent-database/geographies/; 2023.
[61] Stropnik R, et al. Critical materials in PEMFC systems and a LCA analysis for the potential reduction of environmental impacts with EoL strategies. Energy Sci Eng 2019;7(6):2519–39.
[62] Zhang X, et al. Life Cycle Assessment of Power-to-Gas: approaches, system variations and their environmental implications. Appl Energy 2017;190:326–38.
[63] Khan T, Yu M, Waseem M. Review on recent optimization strategies for hybrid renewable energy system with hydrogen technologies: state of the art, trends and future directions. Int J Hydrogen Energy 2022;47(60):25155–201.
[64] Mohseni S, Brent AC. Economic viability assessment of sustainable hydrogen production, storage, and utilisation technologies integrated into on-and off-grid micro-grids: a performance comparison of different meta-heuristics. Int J Hydrogen Energy 2020;45(59):34412–36.
[65] Li B, et al. Sizing of a stand-alone microgrid considering electric power, cooling/heating, hydrogen loads and hydrogen storage degradation. Appl Energy 2017;205:1244–59.
[66] Yudhistira R, Khatiwada D, Sanchez F. A comparative life cycle assessment of lithium-ion and lead-acid batteries for grid energy storage. J Clean Prod 2022;358:131999.
[67] Fthenakis V, et al. Life cycle inventories and life cycle assessment of photovoltaic systems. International Energy Agency (IEA) PVPS Task; 2011. p. 12.
[68] Treyer K, Bauer C. Life cycle inventories of electricity generation and power supply in version 3 of the ecoinvent database—part I: electricity generation. Int J Life Cycle Assess 2016;21:1236–54.
[69] Günkaya Z, et al. Environmental performance of electricity generation based on resources: a life cycle assessment case study in Turkey. Sustainability 2016;8(11):1097.
[70] Mori M, Gutiérrez M, Casero P. Micro-grid design and life-cycle assessment of a mountain hut's stand-alone energy system with hydrogen used for seasonal storage. Int J Hydrogen Energy 2021;46(57):29706–23.
[71] Carmo M, et al. A comprehensive review on PEM water electrolysis. Int J Hydrogen Energy 2013;38(12):4901–34.
[72] Agency IE. World energy balances 2019. 2019.